

# 8.1 Gbps PAM8 Long-Wave IR FSO Transmission using a 9.15- $\mu\text{m}$ Directly-Modulated QCL with an MCT Detector

Mahdieh Joharifar<sup>1</sup>, Mengyao Han<sup>1,2</sup>, Richard Schatz<sup>1</sup>, Rafael Puerta<sup>1,3</sup>, Yan-Ting Sun<sup>1</sup>, Yuchuan Fan<sup>4</sup>, Grégory Maisons<sup>5</sup>, Johan Abautret<sup>5</sup>, Roland Teissier<sup>5</sup>, Lu Zhang<sup>6</sup>, Sandis Spolitis<sup>7,8</sup>, Muguang Wang<sup>2</sup>, Vjaceslavs Bobrovs<sup>7</sup>, Sebastian Lourduos<sup>1</sup>, Xianbin Yu<sup>6</sup>, Sergei Popov<sup>1</sup>, Oskars Ozolins<sup>1,4,7</sup>, Xiaodan Pang<sup>1,4,7</sup>

<sup>1</sup>Department of Applied Physics, KTH Royal Institute of Technology, 106 91 Stockholm, Sweden

<sup>2</sup>Institute of Lightwave Technology, Key Lab of All Optical Network & Advanced Telecommunication Network, Ministry of Education, Beijing Jiaotong University, Beijing 100044, China

<sup>3</sup>Ericsson Research, Ericsson AB, 164 83 Stockholm, Sweden

<sup>4</sup>RISE Research Institutes of Sweden, 16440 Kista, Sweden

<sup>5</sup>mirSense, 2 Bd Thomas Gobert 91120 Palaiseau, France

<sup>6</sup>College of Information Science and Electronic Engineering, Zhejiang University, and Zhejiang Lab, Hangzhou 310027, China

<sup>7</sup>Institute of Telecommunications, Riga Technical University, 1048 Riga, Latvia

<sup>8</sup>Communication Technologies Research Center, Riga Technical University, 1048 Riga, Latvia  
[oskars.ozolins@ri.se](mailto:oskars.ozolins@ri.se), [xiaodan@kth.se](mailto:xiaodan@kth.se)

**Abstract:** We experimentally demonstrate a Long-Wave IR FSO link with a 9.15- $\mu\text{m}$  directly modulated quantum cascade laser at room temperature. Up to 8.1 Gb/s PAM8 transmission over 1.4 meter is achieved with a wideband MCT detector. © 2022 The Author(s)

## 1. Introduction

Free-space optical (FSO) communication systems in the mid-infrared (mid-IR) region, in particular, the two atmospheric transmission windows at the Mid-Wave IR (MWIR, 3-5  $\mu\text{m}$ , 60-100 THz) and the Long-Wave IR (LWIR, 8-12  $\mu\text{m}$ , 25-37 THz), contain rich potential to be a part of the next-generation ICT infrastructure. These two windows are expected to be exploited for long-range FSO applications due to their highly transparent atmospheric channel conditions [1]. Particularly, the laser beam in the LWIR region can propagate through a turbulent atmosphere over far distances, i.e., kilometers, thanks to the low molecular and aerosol scattering and high turbulence robustness at such long wavelengths [2]. With these merits, the LWIR region is currently under-exploited and should be considered a potential candidate for various applications, such as FSO communications, light detection and ranging (LIDAR), and laser propulsion considered for deep-space travel [3]. With the development of the ensemble of semiconductor devices, e.g., quantum optoelectronics devices including the quantum cascade laser (QCL) and quantum cascade detector (QCD) with broad bandwidth operate at room temperature in the mid-IR, compact solid-state FSO transceivers in the MWIR and LWIR become possible [4]. Recently, several LWIR FSO systems comprising QCL and QCD have been demonstrated with both direct modulation and external modulation schemes [4-6]. In these works, however, the stringent requirement for beam collimation and focusing due to the limited conversion efficiency of QCDs hinders the use of high order modulation formats. On the other hand, compared with QCD, though limited in modulation bandwidth, the mercury cadmium telluride (MCT) detectors normally have a broader operational spectral range covering both the MWIR and the LWIR bands. Moreover, owing to the technological maturity, MCT detectors are commercially available with fine-tuned collimation, low thermal noise performance and are often integrated with trans-impedance amplifiers (TIA). With a DM-QCL and a commercial MCT detector, MWIR transmissions of up to 6 Gb/s were recently reported [7].

In this paper, we further explore the characteristics of the wideband MCT detector with a LWIR DM-QCL at 9.15  $\mu\text{m}$ , and report on a high spectral efficiency FSO transmission of up to 8.1 Gb/s 8-level pulse amplitude modulations (PAM8) at 10°C. More specifically, we performed a two-dimensional sweep to identify the optimal operational point considering both the QCL bias and the MCT received power. We achieve bit error rates (BER) below the 6.25% overhead (OH) hard-decision (HD) forward error correction limit [8] with high system stability.

## 2. Experimental configuration

Figure 1(a) shows the experimental setup. For system performance evaluation, we used PAM8 symbol sequences that are mapped from a random binary sequence of >1 million samples generated from the developed digital signal processing (DSP) routine in MATLAB using the Mersenne Twister with a shuffled seed number. To pre-compensate the system bandwidth limit, a root-raised-cosine (RRC) pulse shaping filter with a roll-off factor of 0.15 and a static

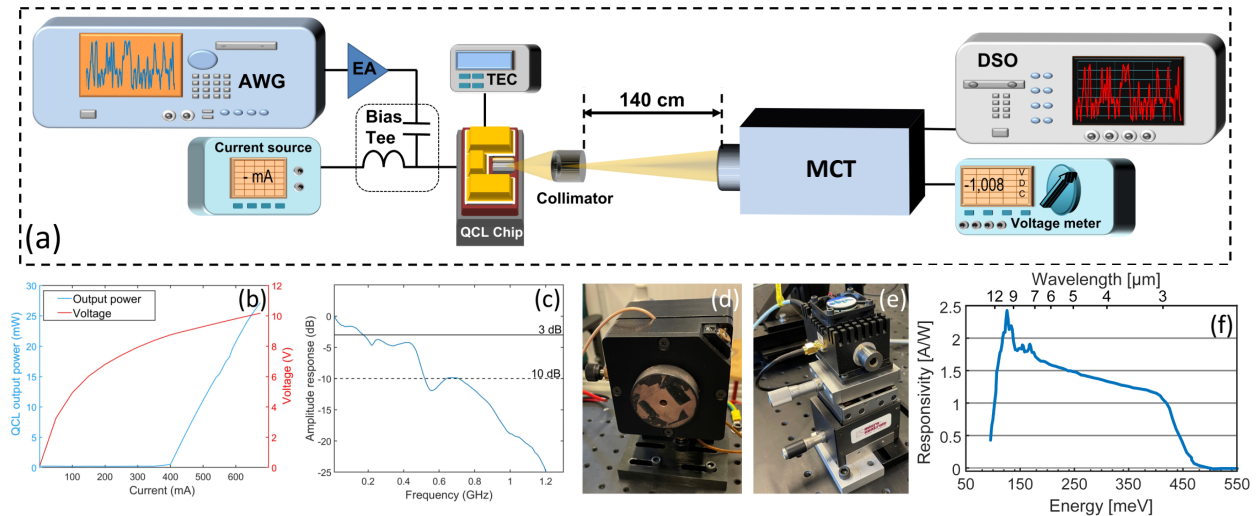


Fig. 1. (a) Experimental setup. (b) P-I-V curve of the 9.15- $\mu\text{m}$  DM-QCL at 10°C. (c). Characterized end-to-end amplitude response, including the QCL, QCD, and all the electrical and RF components. Photos of (d) the QCL mount and (e) the MCT receiver. (f). Spectrum of the MCT receiver responsivity.

2-tap pre-equalization filter are applied to the symbols. A 50 Gsa/s arbitrary waveform generator (AWG) is used to convert the digital samples that are generated offline into the analog domain. The DM-QCL chip with a center wavelength of 9.15  $\mu\text{m}$  is mounted on a water-cooled commercial QCL mount with a Peltier thermoelectric cooler (TEC). Figure 1(b) shows the P-I-V curve of the QCL chip, which is measured at 10°C. At this temperature, the lasing threshold of the laser is around 400 mA, and the saturation appears around 675 mA. The DM-QCL chip is grown by molecular beam epitaxy on an InP cladding. The active region is fabricated by AlInAs/GaInAs structure. The 4-mm single-mode distributed-feedback (DFB) ridge laser processed epi-up on an Aluminum-Nitride submount and obtained through a top metal grating [8]. The laser is biased and modulated through an external bias-tee.

On the receiver side, we use a commercial MCT photo voltage (PV) detector integrated with a TIA. With the help of an IR power meter at the receiver end, we calibrate the received signal power, optimize it, and replace the power meter with the MCT detector to convert the optical signals to electrical signals. A real-time digital storage oscilloscope (DSO) of 40 Gsa/s converts the received electrical signal to digital samples for offline processing. Figure 1 (c) shows the calibrated end-to-end channel amplitude response of the FSO system measured at 10 °C, including the AWG, the DM-QCL, the MCT detector, the DSO, and all the electrical components in between. The end-to-end 3-dB bandwidth is found to be around 170 MHz, and the 10-dB bandwidth is about 520 MHz. One should note that despite the narrow 3-dB bandwidth, the system has a smooth response roll-off. Together with the superior noise performance of the MCT detector and effective post-digital equalization, such a smooth roll-off can support gigabaud-scale signal transmissions. Figure 1 (d) and (e) show the photos of the LWIR transmitter and the MCT detector, respectively. The MCT detector responsivity spectrum is shown in Fig. 1 (f). One can observe that it covers a wide operational spectral range spanning over both MWIR and LWIR, in contrast to QCD that often has a relatively narrower responsivity spectral range [10]. Finally, the signal is processed with a matched filter, a timing recovery and down-sampling process based on maximum variance, a symbol-spaced decision-feedback equalizer (DFE) with 99-feedforward taps and 55-feedback taps, and the BER performance is counted after the offline demodulation.

### 3. Experimental results

We systematically studied the characteristics of the DM-QCL and the MCT detector to identify the optimal operational point for FSO transmission. To do that we performed two consecutive sweeps, namely, a laser bias current sweep with fixed power into the detector, and a received optical power sweep to the MCT detector with the optimal bias point identified in the first sweep. We measured the BER performances of two baud rates, i.e., 2.5 Gbaud and 2.7 Gbaud. The former sweep characterizes the trade-off between modulation depth and the modulation linearity, whereas the later sweep identifies the trade-off between received signal SNR and the detector saturation. Figure 2(a) shows the measured BER results as a function of the laser bias current. The optimal bias point was found around 500 mA to simultaneously obtain a sufficient modulation depth and signal linearity, where both the 2.5 Gbaud and the 2.7 Gbaud PAM8 achieve BER below the 6.25%-OH HD-FEC limit of  $4.5 \times 10^{-3}$ . Figure 2(b)

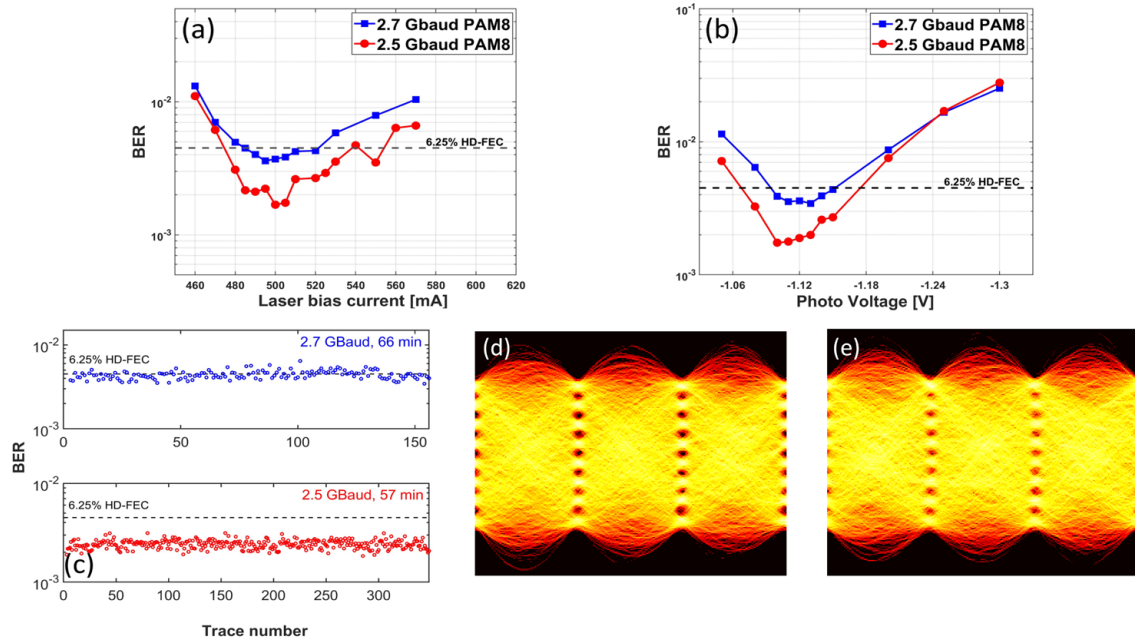


Fig. 2(a). BER results as a function of laser bias for 2.7 Gbaud and 2.5 Gbaud PAM8 at different bias points. (b) BER results as a function of the detector PV for 2.7 Gbaud and 2.5 Gbaud PAM8 at different power points. (c). The stability performance measured for  $\sim 1$  hour. Selected eye diagrams at optimal operational points for (d) 2.5 Gbaud PAM8 and (e) 2.7 Gbaud PAM8, respectively.

shows the measured BER results as a function of the detector photo voltage (PV) with laser biased at 500 mA. The optimal point was found to be around -1.1 V. Figure 2(c) shows the measured stability performance for both baud rates. It shows a stable performance for both the DM-QCL-based transmitter and the MCT IR PV detector. The BER values of 2.5 Gbaud PAM8 are constantly well below the HD-FEC limit, whereas for 2.7 Gbaud some outliers with marginally higher BER than the HD-FEC limit are detected throughout the measurement, due to the fluctuation of signal power caused by vibration. The eye diagrams of 2.5 Gbaud and 2.7 Gbaud PAM8 are shown in Fig. 2 (d) and (e), respectively. Clear eye openings with negligible nonlinear compressions are seen in both baud rates.

#### 4. Conclusion

We demonstrated a LWIR FSO transmission at  $9.15 \mu\text{m}$  with a DM-QCL and a commercial MCT detector. The system supports up to 8.1 Gbaud PAM8 with BER performance below the 6.25%-OH HD-FEC limit with high stability. We consider this work a valuable study contributing to an envisioned fully-connected high-speed LWIR FSO network for the next-generation ICT infrastructure.

#### 5. Acknowledgement

This work was supported in part by the EU H2020 cFLOW Project (828893), in part by the Swedish Research Council (VR) projects 2019-05197, in part by the National Key Research and Development Program of China (2018YFB1801500), in part by the by COST Action CA19111 NEWFOCUS, in part by the ERDF-funded CARAT project (No. 1.1.1.2/VIAA/4/20/660) and in part by the RTU Science Support Fund.

#### 6. References

- [1] A. Delga and L. Leviandier, "Free-space optical communications with quantum cascade lasers," *Proc. SPIE*, 10926 (2019), 1092617.
- [2] J.J. Liu *et al.*, "Mid and long-wave infrared free-space optical communication." *Proc. SPIE*, 11133 (2019), 1113302.
- [3] S. Tochitsky *et al.*, "Megafilament in air formed by self-guided terawatt long-wavelength infrared laser," *Nat. Photon.* 13, 41-46, (2018).
- [4] G. Frédéric *et al.*, "Bridging the 100 GHz-10 THz domain with unipolar quantum optoelectronics," in *Proc. SPIE*(2022), p. 122300A.
- [5] X. Pang *et al.*, "11 Gb/s LWIR FSO Transmission at  $9.6 \mu\text{m}$  using a Directly-Modulated Quantum Cascade Laser and an Uncooled Quantum Cascade Detector," *OFC '22*, Th4B.5.
- [6] H. Dely *et al.*, "10 Gbit  $\text{s}^{-1}$  Free Space Data Transmission at  $9 \mu\text{m}$  Wavelength With Unipolar Quantum Optoelectronics," *Laser & Photonics Reviews*, 16 (2021).
- [7] X. Pang *et al.*, "Up to 6 Gbps Mid-Infrared Free-Space Transmission with a Directly Modulated Quantum Cascade Laser," *ECOC '21*, Tu1B.6.
- [8] L. M. Zhang and F. R. Kschischang, "Staircase Codes With 6% to 33% Overhead," *J. Lightwave Technol.* 32, 1999-2002 (2014).
- [9] M. Carras *et al.*, "Room-temperature continuous-wave metal grating distributed feedback quantum cascade lasers," *Appl. Phys. Lett.* 96, 161105 (2010).
- [10] M. Joharifar *et al.*, "High-Speed  $9.6\text{-}\mu\text{m}$  Long-Wave Infrared Free- Space Transmission with a Directly-Modulated QCL and a Fully-Passive QCD," *J. Lightwave Technol.* 1-7 (2022).